Effect of dispersed particles of aluminum oxide on the degree of defects of the crystalline structure of the chromium coating

Bakhtiyor Mardonov, *Zayniddin* Oripov, *Rashid* Muminov*, *Jamshed* Ravshanov, and *Nodirbek* Jo'rayev

Navoi State University of Mining and Technologies, Navoi, Uzbekistan

Abstract. The paper investigated dependence of the defect of the chromic coating crystal structure containing aluminium oxide microsarches on the current density. The results are presented in graphical form. Likewise, a test of the bonding strength of the coating with the base metal has been carried out. The experiment was carried out by bending a flat sample with a test coating, and the conclusions of the tests are provided.

1 Introduction

The study of defects in the crystal structure of chromium coating was carried out by recording the physical width of the X-ray line, which mainly affects the integral characteristic of defects in the crystal structure - the density of dislocations. As mentioned above, the inclusion of aluminum oxide micro- saws leads to an increase in microhardness, and the increase in microhardness depends on the chromium plating regimes, in fact, the chromium plating regimes affect the amount of aluminum oxide microparticles in the chrome plating. Determining the number of microparticles per unit area of coverage is a more difficult task. However, measuring the crystal structure defects allows us to assess the effect of these particles on the microhardness of the chromium coating. The physical width of the X-ray line (220) was determined by calculating the diagram at half height of the diagram peak. After calculating the width of the diagram, the results of these calculations were used to calculate the dislocation density according to the methodology described X-ray analysis of 30XGSA steel with a chromium coating, obtained at a constant temperature of 55°C and at different current densities. samples were prepared. The results of the study are presented in (Figures 1,2). [1-3, 6-8, 10].

2 Materials and methods

Samples with pure chrome plating were used as reference. As can be seen from the graphs, with the increase of the current density, the defectiveness of the crystalline structure of the chromium coating increases. [3-6, 8, 10, 11].

* Corresponding author: rashid_81@mail.ru

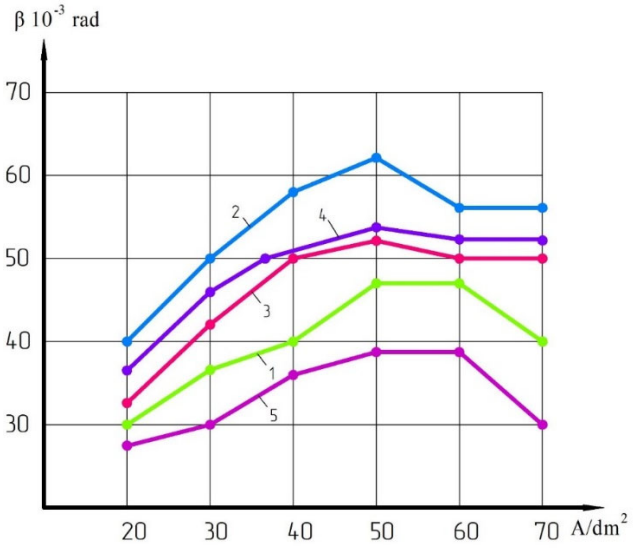

Fig. 1. Aluminum oxide microparticles own into received chrome cover crystalline of the structure defect vine density depends without change.

Electrolytes temperature 55 °C

1- microparticles composition Al_2O_3 -20 g / l
2- microparticles composition Al_2O_3 -40g/l
3- microparticles composition Al_2O_3 -60 g / l
4- microparticles composition Al_2O_3 -80 g / l
5- pure chrome cover.

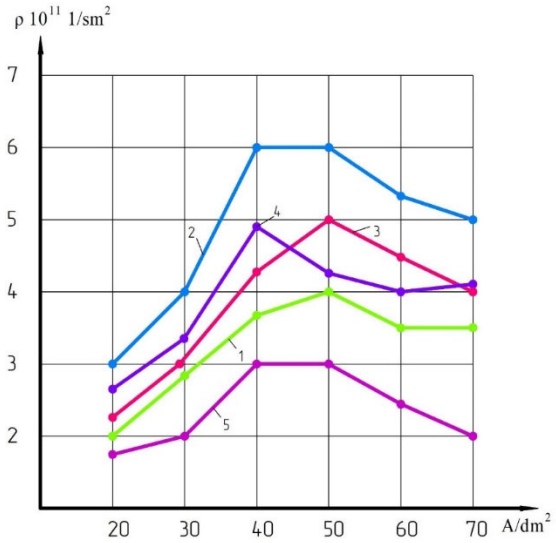

Fig. 2. Aluminum oxide microparticles own into received chrome cover dislocation t political of density vine density depends without change.

Electrolyte temperature 55 °C

1- microparticles content Al_2O_3 -20g/l

2- microparticles content Al_2O_3 -40g/l
3- microparticles content Al_2O_3 -60g/l
4- microparticles content Al_2O_3 -80g/l
5- clean chrome cover

X-ray of the line expansion aluminum oxide microparticles concentration from 40 to 50 g/l. In this case, X-ray of the line the smallest expansion pure chrome in the cover note done _ Chrome in the cover aluminum oxide microparticles similar in composition effect dislocation density in the calculation observed. So that's it to emphasize probably chrome coating microhardness, content from 40 to 50 g/l aluminum oxide microparticles when the most high to value have will be But his maximum value 50A / dm^2 vine density right will come This result is explained by the increase in the amount of aluminum oxide microparticles in the chromium coating, which is manifested in the defect of the crystalline structure of the chromium coating and, accordingly, the increase in the dislocation density [7,9].

3 Results and discussion

Electrolytic chromium crystals are characterized by a small crystal structure with a size of 0.001-0.01 μm. Chromium deposits are characterized by layer-by-layer and characteristic growths observed on the surface when a thick layer of 50 mkm or more is deposited [12].

Chromium- 2 forms a volume-centered cubic lattice with unit cell parameter a= 2.878A and density of 7.1 g/cm^3 during bright chromium plating [13].

Electrolytically deposited chromium contains an average of 0.04-0.5% N_2 and 0.2-0.5% O_2 and composed of a small amount of N_2. Hydrogen is present in the coating as a hydride and in a dissolved state. When the cathode film containing Sch_2O_3 captures the particles, oxygen is precipitated. The presence of N_2 in the composition is the main reason for the brittleness of chrome coatings. After chrome plating as described above, heat treatment is a necessary operation. In the work, it was determined that most of the gases are released at a temperature of 200℃. In addition, the electroplating process b_{vn}creates tensile stress in the chrome plating. The reason for the formation of these stresses is the structural change that causes the reduction of the precipitate volume during the transition from the unstable hexagonal structure to the volume-centered cubic structure. These stresses are removed by heat treatment [14].

Considering the above, roughness parameters R_a of pure chrome coating and composite coatings with aluminum oxide dispersed particles were measured. The results showed that the roughness of the pure chrome coating was 0.12 mkm and the roughness of the composite coating was 0.25 mkm. Thus, the inclusion of aluminum oxide particles creates a greater roughness profile than pure chrome coatings [15].

In addition, a test of the adhesion strength of the coating with the base metal was conducted. The test was carried out by bending a flat sample with a coating. (Figures 1-2). As you can see from these pictures, when the pure chrome coating is bent, wide cracks are formed and the chrome is delaminated from the base metal. it also occurs in composite chrome plating through fine cracks and layer-by-layer migration from the base metal. The cracks indicate that the internal stress is very low compared to that of the pure chromium plating. Metallographic studies have shown that Figures 1-2 have a network of cracks on the surface of the pure chrome plating, which is caused by internal stresses and is a typical condition for chrome plating [16].

The composite chrome finish does not have a mesh of cracks, which should help improve the finish's corrosion resistance. Aluminum oxide particles are evenly distributed in the coating, which allows to obtain a denser structure and reduce the internal floating stress [17].

The rate of corrosion of metals in atmospheric conditions is influenced by the humidity of the air, the impurities in it, and the time the film is on the metal surface. Wetting of the metal surface leads to the formation of an adsorption or phase film of moisture. Adsorption film occurs as a result of moisture condensation when the relative humidity is Ψ = 60+70 %.

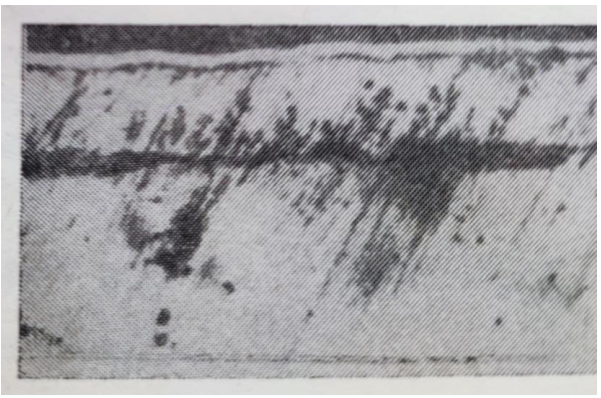

a x150

Fig. 3. Surface after bending test of pure chrome plating.

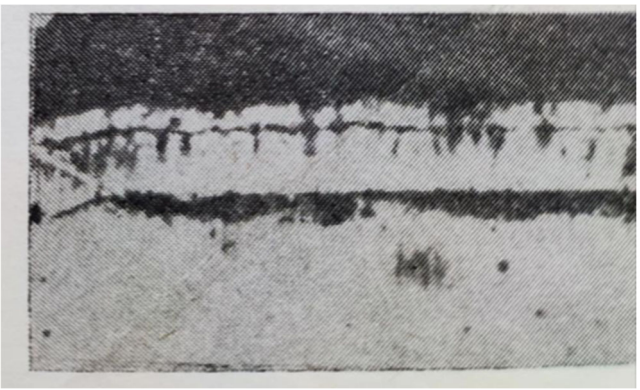

b x150

Fig. 4. Surface of chrome plating with alumina particles after bending test.

The relative humidity at which the adsorption condensation of moisture on the metal surface begins is called the critical humidity. It depends on the condition of the metal and the level of air pollution. In rapid tests, the greatest increase in the corrosion rate is observed when the relative humidity is above the critical condition. Then high adsorption of water vapors and their long storage in metal occurs. Such conditions are created when the relative humidity of the air is close to 100% saturation. In this case, the temperature (40+50) ±℃ is kept at the maximum possible value in atmospheric conditions.

The methodology is based on ST 9.308-85 "Metal and non-metallic inorganic coatings". It specifies methods for accelerated corrosion testing of metallic and non-metallic coatings to obtain comparative data on corrosion resistance and protective capabilities of the coatings. The 0.3 m weather chamber automatically maintains temperature and humidity. A distribution grid inside the chamber ensures uniform conditions and allows the mist to circulate freely around the samples. A contact thermometer connected to the air conditioning chamber performs temperature control.

The given relative humidity of the air in the chamber is achieved by sending air moistened with distilled water. The fan ensures air circulation in the chamber. Samples are hung vertically on hooks. Humidity and temperature control is carried out with a psychrometer. Air is sent to the air preparation chamber by a fan, where it is moistened by spraying distilled water and heated to the desired temperature by heat. Humidified heated air passes through the distribution grid and is distributed throughout the chamber. Samples are attached to discs in the chamber. The distance between samples is 25 mm, the distance to the top and bottom of the chamber is 300 mm. In order for the samples to be evenly sprayed with air, they should be hung at different heights. Temperature - with a thermometer, humidity monitored with a psychrometer. Temperature control is carried out with a contact thermoregulator.

Prepared samples are washed with water, dried, wiped with alcohol and acetone. Samples are marked according to ST 9.905-82. Marked areas of samples are varnish it is protected by covering with paint. A set of samples made of the same metal or alloy and having the same coatings deposited by the same technological process is considered as a variant. For each option, we keep control samples for comparison with the test samples.

After the specified 12-hour period, 3 samples of each option are removed from the test and examined. Control samples and test samples are stored in conditions that prevent corrosion from occurring or increasing, such as in desiccant desiccators. Samples are hung vertically in the chamber on strings or hooks made of polymer or other non-reflective materials. Test samples should occupy 30% of the chamber volume.

The tests were conducted in the following order:

The samples are placed in the chamber, the temperature of the chamber is set to (40±2)℃. Samples are heated 2-3 times higher than the predetermined temperature ℃ and placed in the chamber after the specified temperature is set. The samples are held in the chamber for a period of time sufficient for them to heat up. The essence of this method is that the corrosion process consists in increasing the relative humidity of the air and the temperature without condensing the moisture (Figure 5).

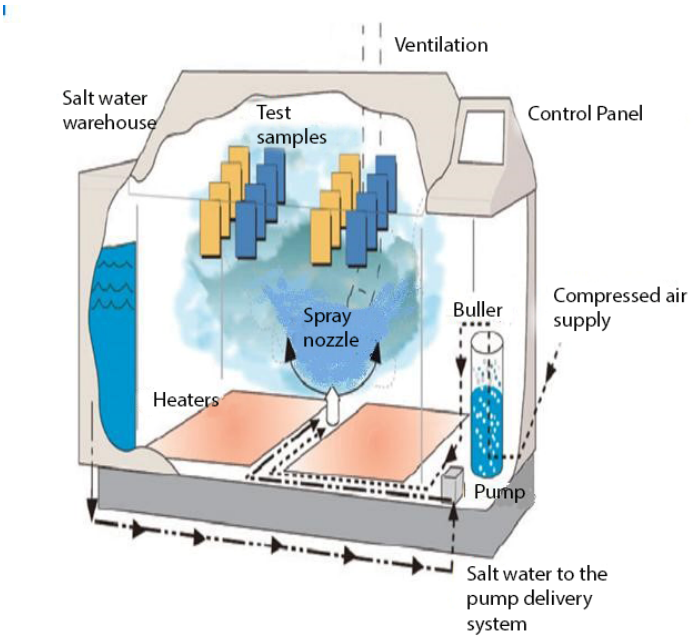

Fig. 5. Climate camera.

After the samples are heated to the specified temperature, relative humidity (93 ± 3%) is created in the air by spraying distilled water into the air flow after the fan. The humidified air impinges on the heating skin, the water droplets turn into vapor, and the vapor-air mixture passes through the gas distribution grid and into the chamber, where it is uniformly sprayed onto the samples. The temperature is adjusted with a contact thermometer using a thermoregulator. Humidity is monitored with psychrometer readings. When the relative humidity is 93-95%, the readings of dry and wet thermometers should be almost the same or the difference should not be greater than 0.1℃. Watering is carried out periodically. In the built-in mode, humidity is maintained at the expense of evaporation of moisture from the surface of the container with water inside the chamber.

Test duration: 12 hours

A sample of 3 of each type of coating in the chamber is removed and inspected at maturity. Before evaluation, the sample surface is washed with a soft brush in hot water with detergent.

4 Conclusions

As a result of the atmospheric corrosion tests, it was found that the mass of the samples decreased by an average of 0.42 m 2 /s after the composite chromium plating, and the mass of the samples decreased by an average of 0.6 m 2 /s after the pure chromium galvanic coating, which is a decrease of 1.5 times. It can be noted that the corrosion process usually starts in the low-density areas of the coating surface, and the high-density structure formed by the penetration of aluminum oxide dispersed particles into the matrix structure resists the spread of corrosion processes into the coating due to the absence of cracks and pores in the coating.

The results obtained are for:

1. Composite chrome coatings were determined experimentally: electrolyte temperature 55 ±2 S, current density 50 A/dm^2.
2. The amount of aluminum oxide dispersed powder in the electrolyte (40 g/l) was determined by planning the experiment.

References

1. B.T. Mardonov, Z.B. Oripov, X.X. Ashurov, International Journal of Advanced Research in Science, Engineering and Technology (IJARSET) **7(8)**, ISSN: 2350-0328 (2020)
2. B.T. Mardonov, Z.B. Oripov, X.X. Ashurov, International Journal of Advanced Research in Science, Engineering and Technology (IJARSET) **8(9)**, ISSN: 2350-0328 (2021)
3. D.A. Kuziev, V.V. Zotov, E.S. Sazankovaa, R.O. Muminov, Eurasian Mining **37(1)**, 76-80 (2022). https://www.doi.org/10.17580/em
4. K.T. Sherov, B.T. Mardonov, O.M. Zharkevich, S. Mirgorodskiy, R. Gabdyssalyk, S.O. Tussupova, N. Smakova, Kh.I. Akhmedov, Y.B. Imanbaev, Journal of Applied Engineering (JAES) Science **18(3)**, 327-332 (2020)
5. A.G. Goltsev, T.B. Kurmangaliyev, K.T. Sherov, M.R. Sikhimbayev, B.N. Absadykov, B.T. Mardonov, A.B. Yessirkepova, News of the National Academy of Sciences of the Republic of Kazakhstan, Series of geology and technical sciences **5(443)**, 63-70 (2020). https://doi.org/10.32014/2020.2518-170X.105
6. R.O. Muminov, G.Ye. Rayxanova, D.A. Kuziev, Ugol **5**, 32-36 (2021). https://www.doi.org/10.18796/0041-5790-2021- 5-32-36

7. Sharif Akhmedov et al, E3S Web of Conferences **390**, 06036 (2023)
8. R.O. Muminov, International Scientific Journal Theoretical & Applied Science **93**, 223-230 (2021) ISSN: 2308-4944 (print) e-ISSN: 2409-0085 (online)
9. I.Y. Yermolenko et al, Nanoscale Research Letters **12(1)**, 352 (2017)
10. J. Sharipov, F. Barakayev, S. Fozilov, Z. Karimova, M. Zaripov, AIP Conference Proceedings **2432**, 050042 (2022)
11. S. Fedorov, J. Sharipov, A. Abrorov, Journal of Physics: Conference Series **1889(2)**, 022079 (2021)
12. Sh.M. Gulyamov, A.N. Yusupbekov, A.O. Ataullaev, K.R. Abdullaeva, Automation. Modern Technologies **1**, 37-42 (2016)
13. Sh.M. Gulyamov, A.N. Yusupbekov, Yu.R. Rashidov, A.O. Ataullaev, Industrial ACS and Controllers **1**, 24-30 (2014)
14. A.N. Yusupbekov, Sh.M. Gulyamov, A.O. Ataullayev, V.H. Shamsutdinova, Journal of Technical University of Gabrovo **51**, 56-60 (2015)
15. Sh.M. Gulyamov, A.N. Yusupbekov, A.O. Ataullaev, Industrial ACS and controllers, **(8)**, 11-16 (2015)
16. A.N. Yusupbekov, A.O. Ataullayev, International Journal of Emerging Technology and Advanced Engineering **5(4)**, 38-44 (2015)
17. A.O. Ataullayev, Journal of Korea Multimedia Society **3-4**, 172-175 (2015)